[4]Guruswamy, G. P., "Unsteady Aerodynamic and Aeroelastic Calculations for Wings Using Euler Equations," *AIAA Journal*, Vol. 28, No. 3, 1990, pp. 461–469.
[5]Tsai, C. J., "A New Concept of Weighting on Schemes for Hyperbolic Equations with Application to Channel Flows," Ph.D. Dissertation, Inst. of Aeronautics and Astronautics, National Cheng Kung Univ., Tainan, Taiwan, ROC, June 1993.
[6]Yee, H. C., and Harten, A., "Implicit TVD Schemes for Hyperbolic Conservation Laws in Curvilinear Coordinates," *AIAA Journal*, Vol. 25, No. 2, 1987, pp. 266–274.
[7]Beam, R. M., and Warming, R. F., "An Implicit Factored Scheme for the Compressible Navier–Stokes Equations," *AIAA Journal*, Vol. 16, No. 4, 1978, pp. 393–402.

Effect of Transverse Shear on Aeroelastic Stability of a Composite Rotor Blade

Sung Nam Jung*
Chonbuk National University,
Chonju 560-756, Republic of Korea
and
Seung Jo Kim†
Seoul National University,
Seoul 151-742, Republic of Korea

Introduction

IN the analysis point of view, the composite rotor blade has typically been analyzed through the one-dimensional beam assumption since the spanwise length of rotor blades is generally much longer than their lateral dimensions. In developing the beam theory, there may be coupling among extension, bending, and torsional deformations. These couplings generally invalidate the Euler–Bernoulli assumption: plane sections remain plane and are perpendicular to the elastic axis. The assumption leads to underestimation of beam displacements, especially in case of bending, because of constant shear distribution across the beam section. Moreover, for a composite beam in bending, this distribution of shear is nearly parabolic (piecewise in general).[1] The use of the shear correction factor (SCF) may be the most economical one for the transverse shear behavior without largely sacrificing the required accuracy of solution. In addition, warping and warping inhibition effects are to be considered in the analysis.[2] Therefore, an appropriate analytical model capturing these behaviors is inevitable to get more enhanced results from the aeroelastic analysis of a composite rotor blade.

Hong and Chopra[3] used the nonlinear kinematic model of Hodges and Dowell[4] and extended it to the case of composite rotor. They used a simplified beam model, in which the transverse shear flexibility was not included in the formulation. Smith and Chopra[5] modified this one to include the transverse shear effects and other secondary structural modeling effects. They focused on the behavior of an elastically tailored composite blade and presented various results for vibratory hub loads of box-beam having different ply configurations, but they did not go further to consider the sectional distribution of shear stresses. To improve the theoretical results, an alternative approach, which has been developed by Jung and Kim[6] for the effects of transverse shear and structural damping on the aeroelastic response of composite rotor blades in hover, involved the usage of SCF to account for the sectional distribution of shear stresses. They showed that the effects of transverse shear and structural damping can have a key role on the flutter boundary of the rotor, but the lay-up structure is confined to symmetric configuration only. In the present work, the formulation of Ref. 6, which considers the effects of transverse shear flexibility, torsion warping, and two-dimensional in-plane behavior, is extended to analyze arbitrary lay-up geometry including antisymmetric configuration. Numerical simulations are performed for a specific antisymmetric configuration to identify the transverse shear behavior on the aeroelastic stability of composite rotor.

Received Sept. 16, 1994; revision received Feb. 6, 1995; accepted for publication Feb. 6, 1995.

*Full-Time Instructor, Department of Aerospace Engineering, Dukjin-Ku. Member AIAA.
†Associate Professor, Department of Aerospace Engineering, Kwanak, Ku. Member AIAA.

Problem Formulation

The rotor structure is idealized as a laminated composite box-beam whose constituent laminae are characterized by different ply orientation angles and different material and thickness properties as depicted in Ref. 6. The deformation of the blade in space is described by u, v, w, and ϕ, which are, respectively, axial, lead-lag, flap, and elastic twist deformations. The total transverse displacements of in-plane and out-of-plane bending are expressed as the sum of the displacement due to bending and the displacement due to shear deformation. The same kinematic relations and constitutive relations that are given by Ref. 6 for the composite box model are used in the present formulation. In case of thin-walled construction of box-beam, the internal shear stresses for the equivalent load applying at shear center are distributed in a form as shown in Fig. 1. Since the distribution of shear strain (or stress) in the load direction of the wall is shown to have nearly parabolic function,[1] an appropriate treatment for the distribution of shear is required for the one-dimensional beam kinematics. Based on the equivalent energy concept, the SCFs are introduced in the present beam formulation to describe the motion. The equilibrium relations for the box-beam composed of orthotropic laminates can be written in the form

$$\begin{Bmatrix} Q_\eta \\ Q_\zeta \end{Bmatrix} = \begin{bmatrix} k_{11}GA_h & 0 \\ 0 & k_{22}GA_v \end{bmatrix} \begin{Bmatrix} v_S' \cos\bar{\theta} + w_S' \sin\bar{\theta} \\ w_S' \cos\bar{\theta} - v_S' \sin\bar{\theta} \end{Bmatrix} \quad (1)$$

where the subscript s represents shear deformation, Q_η and Q_ζ are shear stress resultants in horizontal and vertical directions of box-beam, GA_h and GA_v are the respective shear moduli, k_{11} and k_{22} are the SCFs for in-plane and out-of-plane directions, respectively, and $\bar{\theta}$ is the total geometric pitch angle of blade.

The variation of strain energy δU for the composite blade can be written by

$$\delta U = \int_0^R \iint_A (\sigma_{xx}\delta\varepsilon_{xx} + \sigma_{x\eta}\delta\varepsilon_{x\eta} + \sigma_{x\zeta}\delta\varepsilon_{x\zeta})\, d\eta\, d\zeta\, dx \quad (2)$$

where σ and ε represent engineering stress and engineering strain components, respectively. Substituting the stress-strain and strain-displacement relations, which are described in Ref. 6, into the preceding strain energy equation, and taking Eq. (1) into account, one can obtain the variational form of the strain energy in terms of displacement components. In obtaining the expression of strain energy variation, an ordering scheme is used similar to Ref. 4 to

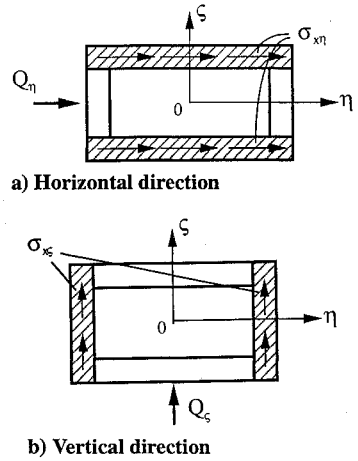

a) Horizontal direction

b) Vertical direction

Fig. 1 Distribution of shear stresses due to applied forces.

systematically eliminate higher order terms. It is assumed that transverse shear deformations v_s and w_s are of order $\varepsilon^{3/2}$ compared with bending deformations v_b and w_b of order ε, and the other field variables have the same order of magnitudes as described in Ref. 4. The kinetic energy for a composite blade can be expressed as the same form for a metal blade except the additional components of kinetic energy originating from the incorporation of transverse shear deformations. The complete details of the kinetic energy expression can be found in Ref. 6. Although the total displacement of the blade is expressed as the sum of the displacement due to bending and shear, the aerodynamic loads induced by the blade motion are also the sum of the loads due to bending and shear deformation. The circulatory aerodynamic forces are obtained from the quasisteady strip theory, and the virtual work done by the nonconservative aerodynamic forces has the form

$$\delta W_e = \int_0^R \left[L_u \delta u + \left(L_{v_b} + L_{v_s}\right)(\delta v_b + \delta v_s) + \left(L_{w_b} + L_{w_s}\right)(\delta w_b + \delta w_s) + M_\phi \delta p\right] \mathrm{d}x \tag{3}$$

where L_u and M_ϕ are the aerodynamic force and moment distributed along the length of the blade in axial and twist directions, L_{v_b} and L_{v_s} denote the edgewise components of aerodynamic forces in bending and shear parts, and L_{w_b} and L_{w_s} denote the flapwise components of aerodynamic loads in bending and shear deformations, respectively. The δp is the virtual rotation of a point on the deformed elastic axis of the beam.

The governing differential equations of motion are obtained by using the extended Hamilton principle. The discretized form in the finite elements can be written by

$$\int_{t_1}^{t_2} \sum_{i=1}^{N_e} (\delta U_i - \delta T_i - \delta W_{ei})\, \mathrm{d}t = 0 \tag{4}$$

where δU, δT, and δW are, respectively, strain energy variation, kinetic energy variation, and external virtual work; N_e is the total number of finite elements; and the subscript i denotes the contribution of an ith element. Each beam element consists of two end nodes and three internal nodes, which results in a total of 23 degrees of freedom including eight transverse shear degrees of freedom. The final nonlinear equations of motion in terms of nodal degrees of freedom $\boldsymbol{q}$ are obtained by using Eq. (4), which results in

$$\boldsymbol{M}(\boldsymbol{q})\ddot{\boldsymbol{q}} + \boldsymbol{C}(\boldsymbol{q})\dot{\boldsymbol{q}} + \boldsymbol{K}(\boldsymbol{q})\boldsymbol{q} = \boldsymbol{F} \tag{5}$$

where $\boldsymbol{M}, \boldsymbol{C}, \boldsymbol{K}$, and $\boldsymbol{F}$ are the global inertia, damping, stiffness matrices, and load vector, respectively. The solution details are described in Ref. 6.

Results and Discussion

Numerical simulations are conducted to see the effects of transverse shear deformations on the aeroelastic behavior of composite rotor. The results are obtained for a hingeless rotor blade with Lock number $\gamma = 5.0$, solidity ratio $\sigma = 0.1$, chord-to-span ratio $c/R = 0.08$, and zero precone. The chordwise offsets of the center of mass, aerodynamic center, and tension center from the elastic axis are assumed to be zero. The airfoil characteristics used were $c_l = 5.7\alpha$, $c_d = 0.01$, and $c_{\mathrm{mac}} = 0$. The blade structure is represented by a laminated composite box-beam composed of four walls. Five normal modes (two flap, two lag, and one torsion) calculated at deformed equilibrium position of the blade are used to perform the stability analysis. A baseline blade configuration has stiff in-plane property as the first flap frequency $\omega_w = 1.15$ /rev, the first lag frequency $\omega_v = 1.5$ /rev, and the first torsion frequency $\omega_\phi = 5.0$. Stability results are obtained for an antisymmetric configuration, where the ply lay-ups on opposite walls with respect to geometric center of box section are of reversed orientation with each other. However, each of the four laminates has symmetric lay-ups about the respective middle surfaces: the laminae for the central one-third of thickness are laid up at arbitrary angle Λ, but the laminae for the remaining two-thirds of the thickness are all oriented at zero angles. The length R of the rotor is 4.42 m, and the cross section of the beam has an outside dimension of 0.178 m width by 0.051 m height with 8.89×10^{-3} m thick. The mechanical properties of composites used herein are $E_{11} = 206.7$ GPa, $E_{22} = 20.67$ GPa, $G_{12} = G_{13} = 8.270$ GPa, $\nu_{12} = 0.3$, and $\rho = 1,742$ kg/m^3. The calculated SCFs in this model are $k_{11} = 0.7377$ and $k_{22} = 0.1264$.

Figures 2 and 3 show the root locus plots with changing ply angle Λ for the first lag and flap modes, respectively, at a thrust level of $C_T/\sigma = 0.1$. For this antisymmetric configuration, the major coupling terms affecting the composites behavior are bending-shear and extension-torsion couplings. Unlike the stability results of symmetric configurations displayed in Ref. 6, where only slight changes of aeroelastic roots are presented, the stability roots of the blade having antisymmetric lay-ups are shown to be largely changed by these coupling terms. The effect of transverse shear on the lag mode eigenvalues is quite large on the damping of the mode as seen in Fig. 2. With the inclusion of transverse shear, the instability occurs at layer angles of 10–30 deg. In general, the transverse shear tends to lower the frequency of the mode and destabilizes the motion in a large scale, but the effect is reversed at Λ of -10 to -30 deg. This fact is closely related to the following results of Fig. 3. Figure 3 depicts that the transverse shear effect on the flap mode frequency is quite significant. Positive Λ stiffens the flap mode and negative Λ softens this one. Very low flap frequency of the blade is obtained for Λ of -10 to -20 deg. The blade seems to be in a statically unstable state (torsional divergence) at these ply angles. This critical

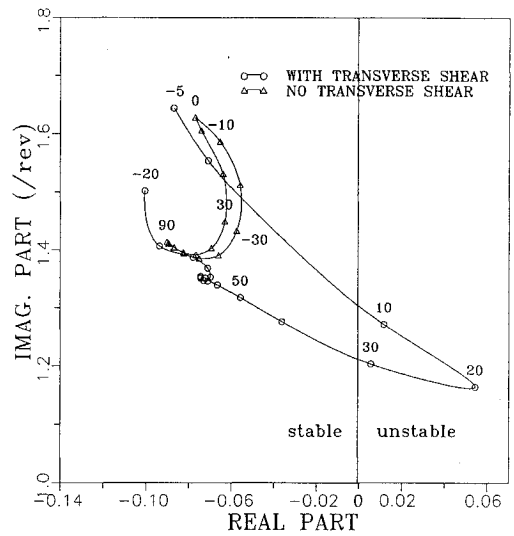

Fig. 2 Transverse shear effects on the stability solution of the first lag mode in antisymmetric configuration.

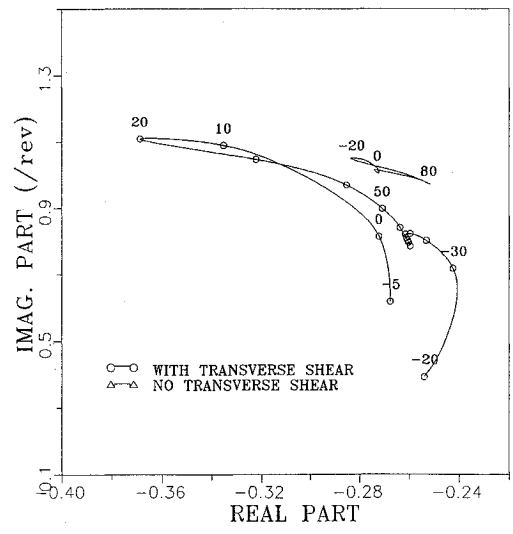

Fig. 3 Transverse shear effects on the stability solution of the first flap mode in antisymmetric configuration.

condition is thought to be brought about by the unusual results of lag mode eigenvalues at layer angles of −10 to −30 deg.

Concluding Remarks

In this work, the effects of transverse shear on the aeroelastic analysis of a composite rotor having antisymmetric configuration have been investigated by using the finite element method. The results shown in this article reveal that, for this type of configuration, the incorporation of transverse shear influenced the system on both the frequency and damping in a dramatic manner: instabilities occurred at several ply orientation angles. So it is vital from the analysis that the transverse shear flexibility (considering the distribution of shear) should be kept for the analysis of composite rotor to get more enhanced results.

References

[1]Whitney, J. M., "Shear Correction Factors for Orthotropic Laminates Under Static Load," *Journal of Applied Mechanics*, Vol. 40, March 1973, pp. 302–304.

[2]Rehfield, L. W., Atilgan, A. R., and Hodges, D. H., "Nonclassical Behavior of Thin-Walled Composite Beams with Closed Cross Sections," *Journal of the American Helicopter Society*, Vol. 35, No. 2, 1990, pp. 42–50.

[3]Hong, C. H., and Chopra, I., "Aeroelastic Stability Analysis of a Composite Rotor Blade," *Journal of the American Helicopter Society*, Vol. 30, No. 2, 1985, pp. 57–67.

[4]Hodges, D. H., and Dowell, E. H., "Nonlinear Equations of Motion for the Elastic Bending and Torsion of Twisted Nonuniform Blades," NASA TN D-7818, Dec. 1974.

[5]Smith, E. C., and Chopra, I., "Aeroelastic Response, Loads and Stability of a Composite Rotor in Forward Flight," *AIAA Journal*, Vol. 31, No. 7, 1993, pp. 1265–1273.

[6]Jung, S. N., and Kim, S. J., "Aeroelastic Response of Composite Rotor Blades Considering Transverse Shear and Structural Damping," *AIAA Journal*, Vol. 32, No. 4, 1994, pp. 820–827.

Effects of Boundary Conditions on Postbuckling of Compressed, Symmetrically Laminated Thick Plates

Erasmo Carrera* and Michele Villani†
Politecnico di Torino, 10129 Torino, Italy

I. Introduction

CURRENT metal aircraft design practices allow the skin of some structural components (e.g., fuselage, wing, and stabilizer panels) to buckle at load levels below the design ultimate loading condition. In fact, these structural elements are designed to have a postbuckling strength; evidently a better understanding of the postbuckling behavior of composite panels constitutes an essential requirement toward a rational employment of their strength. Both their ultimate loading conditions and failure characteristics must be well understood.

Boundary conditions play a fundamental role in nonlinear analysis of laminated panels as well as of metallic, isotropic ones. In fact, buckling and postbuckling behavior is very much affected by them. Many examples and exhaustive overviews can be found in the report by Leissa[1] for buckling and in the Chia's book[2] for postbuckling. These two works discuss results related to the classical Kirchhoff's plate approximations classical lamination theory (CLT). The interest in these subjects is also displayed by the many experimental research activities that were carried out in many laboratories all over the world; as example and for literature we cite the work by Starnes et al.[3] and more recently that by Chai et al.[4]

Usually these experiments are very expensive and the cost of a parametric study becomes prohibitive. Laminated structures exhibit higher transverse deformability in respect to that of metallic ones. In fact, thickness and orthotropic ratio increasing the shear deformation cannot be neglected; further it assumes much more importance in the large deflections field. Some aspects related to first shear deformation theory (FSDT) and nonlinear analysis of composite plates were overviewed by Chia,[5] whereas effects related to higher order shear deformation theory (HSDT) have been recently considered and reviewed by Librescu and Stein[6] and Librescu and Chang.[7] Because of both the limitations of the analytical methods as those in Refs. 1–7 and the high cost of experiments, only a limited amount of data has been published to describe the postbuckling behavior of composite flat panels. These data are even less when shear deformable plates are considered and different boundary conditions are treated. The progress made by approximated methods of the computational mechanics and particularly by the finite element method (FEM) as tools to trace the nonlinear response of many different problems has been recently pointed out by Crisfield.[8] Furthermore the difficulties and/or limitations of the analytical methods to consider different geometrical and mechanical boundary conditions are easily subjugated. On the other hand FEM formulations (especially when concern plates and shells) are very often affected by numerical deficiencies as locking. Fortunately these weaknesses can be overcome by implementation of some strategies as those discussed by Dvorkin and Bathe.[9]

The present work is a sequel to the work of Carrera[10–15] directed to investigate composite plates by FEM. It uses a shear deformable plate finite element of Reissner–Mindlin type. Nonlinearities of von Kármán type are included (large rotations, large strains, and material nonlinearities are not considered). To obtain low bandwidth of FEM stiffnesses matrices, the simple four node plate element $Q4$ is employed. The numerical efficiency of this element has been reached by application of assumed shear strain field concept discussed by Dvorkin and Bathe[9] among the others. The multilayered formulation of this element was proposed by Carrera in Refs. 13 and 15 and implemented in the FEM code MATCO, which is available at Dipartimento di Ingegneria Aeronautica e Spaziale. Elastic flat plates subjected to static conservative loads are considered. Symmetrically anisotropic laminated plates loaded by in-plane axial compression are analyzed. As novelty in respect to the previous works, herein the attention is focused to the effects of boundary conditions. In particular the effects related to stiffeners are studied and the cases of constant distribution of the displacements at the plate loaded edges are compared with results related to a constant distribution of the load at the same edges.

II. Outlines of the Used Finite Element Model

Consider an elastic body subjected to static loads and under prescribed boundary conditions. If the body is assumed to execute an arbitrary set of infinitesimal virtual displacements, from the actual configuration, the principle of virtual displacements states

$$\delta\Psi = \delta W \tag{1}$$

where $\delta\Psi$ is the virtual variation of the strain energy and δW is the virtual variation of the external work. Upon application of FEM approximations, the variational equation (1) then reduces to a nonlinear set of algebraic equations that we write in the two following equivalent forms[12]:

$$\{\varphi(\{q\},\{p\})\} = 0; \qquad [K_S(\{q\})]\{q\} = \{p\} \tag{2}$$

where $\{q\}$ is the n-dimensional vector of the nodal displacements and/or rotations, $\{\varphi\}$ is the n-dimensional vector of the resultant nodal forces (inner plus external forces), $\{p\}$ is the n-dimensional vector of the nodal forces equivalent to the external loads (which is assumed deformation independent), and $[K_S]$ is the secant stiffness matrix. (Brace and square brackets denote vectors and matrices, respectively. We refer to the displacements formulation of the FEM.) Equation (2) constitutes the point of departure for finite element

Received July 21, 1994; revision received March 15, 1995; accepted for publication March 15, 1995.

*Research Engineer, Dipartimento di Ingegneria Aeronautica e Spaziale, Corso Duca degli Abruzzi, 24. Member AIAA.

†Doctoral Student, Dipartimento di Ingegneria Aeronautica e Spaziale, Corso Duca degli Abruzzi, 24.